Dissimilar collective decay and directional emission from two quantum emitters

P. Solano [1,*] P. Barberis-Blostein,[2] and K. Sinha [3,†]

[1]*Departamento de Física, Facultad de Ciencias Físicas y Matemáticas, Universidad de Concepción, Concepción, Chile*

[2]*Instituto de Investigaciones en Matemáticas Aplicadas y en Sistemas, Universidad Nacional Autónoma de México, Ciudad Universitaria, 04510, DF, México*

[3]*School of Electrical, Computer and Energy Engineering, Arizona State University, Tempe, Arizona 85287-5706, USA*

We study a system of two distant quantum emitters coupled via a one-dimensional waveguide where the electromagnetic field has a direction-dependent velocity. As a consequence, the onset of collective emission is nonsimultaneous, and, for appropriate parameters, radiation could be enhanced for one of the emitters while inhibited for the other. Interference effects enable the system to radiate in a preferential direction depending on the atomic state and the field propagation phases. We characterize such directional emission as a function of various parameters, delineating the conditions for optimal directionality.

I. INTRODUCTION

Engineering atom-photon interactions by manipulating electromagnetic (EM) fields is a significant aspect of design and implementation of quantum technologies [1–3]. For instance, reducing the mode volume of the EM field enhances the light-matter coupling [4] and controlling the field polarization allows for chiral interactions between quantum emitters with polarization-dependent transitions [5]. Current platforms allow one to change yet another property of the EM field: its propagation velocity [6–8]. In particular, one can envision the possibility of having an EM field with unequal velocities when propagating to the left or to the right, here referred to as *anisotachy*.[1] Such feature is, as yet, an unexplored aspect of quantum optical systems, which could be implemented with state-of-the art nonreciprocal components [9,10]. Since the propagation velocity is an essential ingredient in connecting the distant parts of a larger system, the effects of anisotachy are expected to appear when measuring properties that depend on the interaction between delocalized subsystems, such as quantum correlations.

Quantum correlations among emitters can collectively enhance or inhibit light absorption and emission [11]. For example, a collection of emitters can radiate faster or slower than individual ones depending on their correlations, phenomena known as super- and subradiance respectively.[2] These effects have been extensively studied both theoretically [11–16] and experimentally across various platforms [17–29].

Recent works have proposed, and implemented [30], collective effects for controlling the direction of emission using the nonlocal correlations between two emitters, with potential applications in quantum information processing and quantum error correction [31–34].

In this work we propose a system comprising of two distant quantum emitters or atoms coupled to a one-dimensional waveguide with an effective direction-dependent field velocity, or anisotachy. As we will show, a direction-dependent time delay can allow two correlated emitters to exhibit disparate collective effects such that while the decay of one atom is enhanced, the decay of the other is inhibited. In such a system, interference effects in the radiated field lead to a directional emission. We characterize such directional emission as a function of initial states of the emitters, field propagation phases, and the waveguide coupling efficiency. Our results demonstrate that collective directional emission is a rather prevalent quantum optical phenomenon that needs further exploration, to understand its advantages, limitations, and dependence on a broader set of parameters. We first present a theoretical model of the system, describing the disparate cooperative decay dynamics of the emitters and the radiated field intensity in the presence of anisotachy. We then characterize the optimum conditions for directional emission. Finally we discuss the experimental feasibility and give a brief outlook of the phenomena.

II. MODEL

Let us consider two two-level quantum emitters coupled to the EM field modes of a waveguide. The field modes propagate through different waveguide with unequal velocities on the left and the right, as shown in Fig. 1, leading to an effective anisotachy.

The Hamiltonian for the system is given as $H = H_E + H_F + H_{EF}$, where $H_E = \sum_{m=1,2} \hbar\omega_0 \hat{\sigma}_m^+ \hat{\sigma}_m^-$ is the Hamiltonian for the emitters, with $[\hat{\sigma}_m^+, \hat{\sigma}_m^-]$ as the raising

---

*psolano@udec.cl

†kanu.sinha@asu.edu

[1]The term *anisotachy* comprises the Greek words *aniso* for unequal and *tachytita* for velocity.

[2]In the context of this paper, super- and subradiance indicate the instantaneous rate of atomic excitation decay being faster or slower than independent decay.
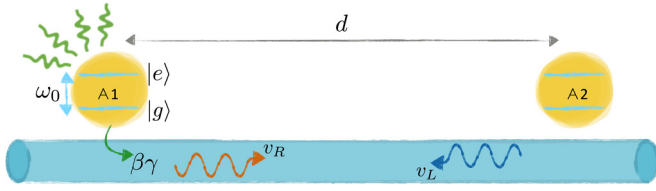
FIG. 1. Schematic representation of two two-level atoms coupled to a waveguide with an interatomic separation d. The waveguide is such that the left (right) propagating modes have a velocity v_L (v_R). The atoms have a resonance frequency ω_0 and a decay rate γ, and couple to the waveguide with a coupling efficiency β.

and lowering operators for the mth atom. $H_F = \int_0^\infty d\omega\, \hbar\omega\{\hat{a}_R^\dagger(\omega)\hat{a}_R(\omega) + \hat{a}_L^\dagger(\omega)\hat{a}_L(\omega)\}$, corresponds to the Hamiltonian for the guided modes of the waveguide, with $\hat{a}_{L(R)}^{(\dagger)}$ as the bosonic operators for the left (right) propagating modes. The interaction Hamiltonian in the interaction picture with respect to the free Hamiltonians $H_E + H_F$ is [35,36]

$$\tilde{H}_{EF} = \sum_{m=1,2} \int_0^\infty d\omega\, \hbar g(\omega)\{\hat{\sigma}_m^+[\hat{a}_R(\omega)e^{ik_R x_m} + \hat{a}_L(\omega)e^{-ik_L x_m}]e^{-i(\omega-\omega_0)t} + \text{H.c.}\}, \quad (1)$$

where $x_1 = -x_2 = -d/2$ denotes the position of the emitters, $g(\omega)$ represents the atom-field coupling strength and $k_{L,R} \equiv \omega/v_{L,R}$ corresponds to the asymmetric left and right wave numbers. This Hamiltonian, in the weak coupling regime and

rotating-wave approximation, accurately describe the system. Considering the initial state of the system with the emitters being in the single excitation subspace and the field in vacuum,

$$|\Psi(t)\rangle = \left\{ \sum_{m=1,2} c_m(t)\hat{\sigma}_m^+ + \int_0^\infty d\omega\, [c_R(\omega, t)\hat{a}_R^\dagger(\omega) + c_L(\omega, t)\hat{a}_L^\dagger(\omega)] \right\} |gg\rangle \otimes |[0]\rangle, \quad (2)$$

one can derive the equations of motion for the atomic coefficients, c_1 and c_2, using a Wigner-Weisskopf approach as (see Appendix A for details)

$$\dot{c}_{1(2)}(t) = -\frac{\gamma}{2}\Big[c_{1(2)}(t) + \beta c_{2(1)}(t - T_{L(R)}) \times \Theta(t - T_{L(R)})e^{i\omega_0 T_{L(R)}}\Big]. \quad (3)$$

Here γ is the total spontaneous emission rate, $\beta\gamma = 4\pi|g(\omega_0)|^2$ is the decay rate into the guided modes, and $T_{R(L)} = d/v_{R(L)}$ is the propagation time of the field traveling right (left) from one emitter to the other.

III. DYNAMICS

Let us consider the initial state of the emitters to be $|\Psi_0\rangle \equiv c_1(0)|eg\rangle + c_2(0)|ge\rangle$. The equations of motion [Eq. (3)] can be solved to obtain (see Appendix B):

$$c_{1(2)}(t) = \underbrace{\sum_{n=0}^\infty c_{1(2)}(0)e^{i2n\phi}\frac{(\beta\gamma/2)^{2n}}{(2n)!}(t - 2nT)^{2n}e^{-\gamma(t-2nT)/2}\Theta(t - 2nT)}_{\text{Even number of trips between atoms}}$$

$$- \underbrace{\sum_{n=0}^\infty c_{2(1)}(0)e^{i2n\phi + i\phi_{L(R)}}\frac{(\beta\gamma/2)^{2n+1}}{(2n+1)!}(t - 2nT - T_{L(R)})^{2n+1}e^{-\gamma(t-2nT-T_{L(R)})/2}\Theta(t - 2nT - T_{L(R)})}_{\text{Odd number of trips between atoms}}, \quad (4)$$

where $\phi_{R(L)} = \omega_0 T_{R(L)}$ is the phase acquired by the resonant field upon propagation between the emitters, and $T = (T_R + T_L)/2$, $v = (v_R + v_L)/2$, $\phi = (\phi_R + \phi_L)/2$ are the average propagation time, velocity, and phase, respectively.[3] The first term in the equation above represents the modification of atomic decay after n round trips of the field between the emitters. The second term represents an odd number of trips $(2n + 1)$ from one emitter to the other. The directional propagation phase ($\phi_{R(L)}$), together with the phase from the atomic coefficients ($c_{2(1)}$), determines the constructive or destructive nature of interference between the two terms. In the absence of anisotachy, Eq. (4) reduces to previous results [37,39].

Figure 2(a) shows the decay of the atomic excitation coefficients as a function of time. Destructive (constructive) interference in the left (right) propagating modes leads to

an inhibited decay of atom A1 and enhanced decay of atom A2, after the field from one atom reaches the other. One can thus interpret collective decay as a mutually stimulated emission process, as is evident from the series expansion in Eq. (4). For a negligible separation between emitters ($T \to 0$), the series converges to yield the standard superradiant exponential decay. In the presence of delay, the resulting dynamics is more precisely described as a cascade of stimulated emission processes [42]. For instance, the field from one emitter can stimulate emission of the other, leading to a nonexponential decay that is faster than superradiance [37,40,41,43], or completely suppress its emission, leading to bound states in the continuum (BIC) [38,44]. More generally, this effect can accelerate the decay of one atom while slowing the decay of the other, as shown in Fig. 2(a). This demonstrates that the phenomena of super- and subradiance extends beyond the system as a whole, and it can be used for an effective description of local atom-photon interference effects.

---

[3]In the absence of anisotachy, it simplifies to previous results of collective radiation in the presence of delay [37–41].

TABLE I. Some representative examples of dissimilar collective decay for different atomic and field propagation phases.

ϕ_L	ϕ_R	$\phi_{A1} - \phi_{A2}$	Atom 1	Atom 2	
$2n\pi$	$(2m+1)\pi$	0	Enhanced	Inhibited	Anisotachy
		π	Inhibited	Enhanced	required
$(2n+1)\pi$	$2m\pi$	0	Inhibited	Enhanced	Anisotachy
		π	Enhanced	Inhibited	required
$(n+\frac{1}{2})\pi$	$(m+\frac{1}{2})\pi$	$\frac{\pi}{2}$	Inhibited	Enhanced	No anisotachy
		$-\frac{\pi}{2}$	Enhanced	Inhibited	required

One can note a few salient features of the collective atomic dynamics from the above equation:

(1) Each term in the series expansion can be interpreted as multiple partial reflections of a field wave packet bouncing between the atoms at signaling times $t = 2nd/v$ and $2nd/v + d/v_{L(R)}$, as denoted by the theta functions [$\Theta(t - 2nd/v)$ and $\Theta(t - 2nd/v - d/v_{L(R)})$]. This offers the intuition that the collective decay dynamics arises from a cascade of stimulated emission processes as the field emitted by the each of the atoms propagates back and forth between them.

(2) The interference phase for all partial reflections is determined by the phase factors $c_{1(2)}(0)e^{i2n\phi}$ and

$c_{2(1)}(0)e^{i2n\phi + i\phi_{L(R)}}$, which is a combination of the atomic and field propagation phases. Each successive term comes with an additional factor of the atom-waveguide coupling strength $\beta\gamma/2$.

(3) The propagation phases $\phi_{L(R)}$ can be different in the presence of anisotachy, which can make the contribution from the second term to the collective dynamics different for the two atoms, thus leading to dissimilar collective behavior. We summarize a few example cases of such behavior in Table I.

The EM field intensity emitted by the system, as a function of position x and time t, can be evaluated as $I(x,t) = \frac{\epsilon_0 c}{2}\langle\Psi(t)|\hat{E}^\dagger(x,t)\hat{E}(x,t)|\Psi(t)\rangle$[4] (see Appendix C):

$$\frac{I(x,t)}{I_0} = \left| \left\{ \underbrace{C_1(t, [x+d/2]/v_L)e^{-i\omega_0(x+d/2)/v_L}}_{\text{Atom 1 left light cone}} + \underbrace{C_2(t, [x-d/2]/v_L)e^{-i\omega_0(x-d/2)/v_L}}_{\text{Atom 2 left light cone}} \right. \right.$$

$$\left. \left. + \underbrace{C_1(t, -[x+d/2]/v_R)e^{i\omega_0(x+d/2)/v_R}}_{\text{Atom 1 right light cone}} + \underbrace{C_2(t, -[x-d/2]/v_R)e^{i\omega_0(x-d/2)/v_R}}_{\text{Atom 2 right light cone}} \right\} \right|^2, \quad (5)$$

where we have redefined the atomic excitation coefficients $C_i(t, \tau) = c_i(t + \tau)\zeta(t, \tau)$ to explicitly include the causal dynamics in the notation, with $\zeta(t_1, t_2) \equiv \Theta(t_1 + t_2) - \Theta(t_2)$. The first (last) two terms above correspond to the left- (right-) going light cones emitted from the atoms A1 and A2. Figure 2(b) shows the radiated intensity with the emitted fields destructively (constructively) interfering to the left (right) leading to almost perfect directional emission.

IV. DIRECTIONAL EMISSION

We characterize the probability of emitting the photon into the right (left) propagating mode by $P_{R(L)}(\Psi_0) = \lim_{t\to\infty} \int_0^\infty d\omega |c_{R(L)}(\omega, t)|^2$, with $P_{R(L)}(\Psi_0)$ as an explicit function of the initial state $|\Psi_0\rangle$ (see Appendix D). We focus here on the limit of small atomic separation $\gamma T \ll 1$ such that retardation effects are negligible. For convenience we write the initial condition as $c_1(0) = \cos\theta e^{i\phi_{A1}}$ and $c_2(0) = \sin\theta e^{i\phi_{A2}}$. The probability of emitting in a particular direction is a function of four parameters: the coupling efficiency β, the

average propagation phase ϕ; the initial atomic populations parametrized by θ; and the difference between the relative atomic and propagation phases $\Delta\phi = (\phi_{A1} - \phi_{A2}) + (\phi_R - \phi_L)/2$. For a given experimental realization, the parameters β and ϕ would be fixed, and the variable atomic parameters θ and $\Delta\phi$ would determine the directionality of emission.

The directional emission of the system can be characterized by $\chi = (P_R - P_L)/(P_R + P_L)$, which can be calculated explicitly as (see Appendix D)

$$\chi(\Psi_0) = -\frac{\beta\sin\phi}{P_{\text{tot}}}\left(\frac{\sin\Delta\phi\sin 2\theta + \beta\cos 2\theta\sin\phi}{1 + (\beta\sin\phi)^2}\right), \quad (6)$$

where $P_{\text{tot}} = P_R + P_L$ is the total probability of emitting into the waveguide:

$$P_{\text{tot}}(\Psi_0) = \beta\left[\frac{1 - \beta\cos^2\phi - (\beta - 1)\cos\Delta\phi\cos\phi\sin 2\theta}{1 - (\beta\cos\phi)^2}\right]. \quad (7)$$

We note from the above that $P_{\text{tot}} = \beta$ only for $\phi = (n + \frac{1}{2})\pi$, more generally, the interference in the field enhances or inhibits the effective coupling efficiency between the emitters and the waveguide. Equation (6) shows that the emission is typically directional for most values of $\Delta\phi$ and $\phi \neq N\pi$,

---

[4]Here $\hat{E}(x,t) = \int_0^\infty dk\, \mathcal{E}_k[\hat{a}_L(k)e^{-ik_L x} + \hat{a}_R(k)e^{ik_R x}]e^{-i\omega t}$ is the electric field operator, and we have assumed $\mathcal{E}_k \approx \mathcal{E}_{k_0}$ to be constant near the atomic resonance frequency.
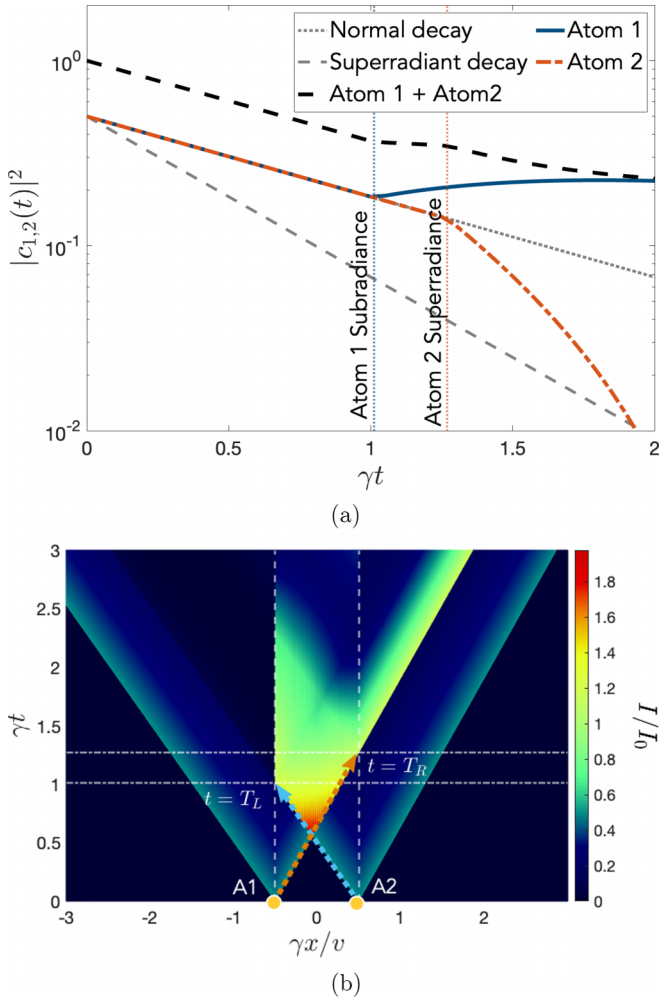
FIG. 2. Atomic excitation probability and intensity dynamics for emitters prepared initially in the symmetric state $|\Phi_0\rangle = \frac{1}{\sqrt{2}}(|eg\rangle + |ge\rangle)$, with $\phi_L = \pi$ and $\phi_R = 2\pi$. (a) The blue solid and red dash-dotted curves represent the populations of atoms A1 and A2, respectively, with the dotted vertical lines indicating the onset of collective emission. The gray dotted and dashed curves represent standard individual and superradiant decay, respectively. The thick dashed line represents the excitation probability of the entire atomic system, which tends to subradiance. (b) Intensity of the radiated field as a function of spacetime. The vertical dashed lines indicate the position of the two atoms while the horizontal dash-dotted lines represent the times $t = T_L$ and $t = T_R$. Here we have chosen the dimensionless atomic separation $\gamma d/c \approx 1$, propagation velocities $v_L/c \approx 0.988$ and $v_R/c \approx 0.788$, $\omega_0/\gamma \approx 500$ and coupling efficiency $\beta \approx 1$.

$N \in \mathbb{N}$. This indicates a prevalence of directional emission in quantum optical systems.

Figure 3 shows the directionality of photon emission χ as a function of the parameters of the initial atomic state for the optimum directionality condition $\phi = (n + \frac{1}{2})\pi$, for two particular waveguide coupling efficiencies ($\beta = 1$ and 0.01). Considering two orthogonal entangled atomic states $|\Psi_{a(b)}\rangle = \frac{1}{\sqrt{2}}(|eg\rangle + e^{i\varphi_{a(b)}}|ge\rangle)$ with $\varphi_a - \varphi_b = \pi$, we obtain a directional parameter value $\chi_{a(b)} = \sin(\phi_R - \phi_L - \varphi_{a(b)})/(1 + \beta^2)$. It can be thus seen that appropriately manipu-
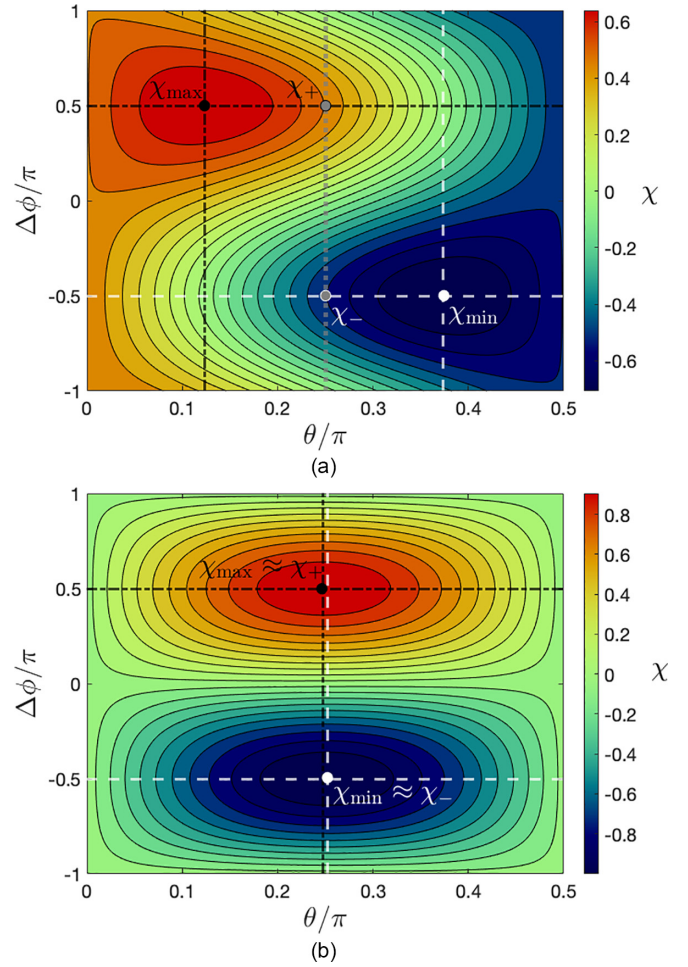

FIG. 3. Directionality parameter χ as a function of the initial atomic state parameters, for waveguide coupling efficiencies of (a) $\beta = 1$ (b) $\beta = 0.01$. The propagation phase is fixed to be $\phi = \pi/2$ and the atomic separation is considered to be in the nonretarded regime ($\gamma T \ll 1$). (a) For $\beta = 1$, the maximum directionality is obtained for $\theta = \pi/8$ and $\Delta\phi = \pm\pi/2$ with a maximum and minimum χ values of $\chi_{\max} = -\chi_{\min} = 1/\sqrt{2}$. The gray points indicate directional emission obtained for initial states $|eg\rangle \pm i|ge\rangle$ with a $\chi_\pm = \pm 1/2$ [32]. (b) For $\beta = 0.01$ the directional parameter can be as large as $\chi_{\max} = -\chi_{\min} \approx 0.999$.

lating the relative field propagation phase ($\phi_R - \phi_L$) can allow one to distinguish any two orthogonal maximally entangled states in the single excitation subspace based on the direction of emission, as illustrated by the points χ_+ and χ_- in Fig. 3.

We note that the directional emission from an entangled state benefits from $\beta < 1$ as can be seen from comparing Figs. 3(a) and 3(b). This can be understood from the series expansions in Eqs. (4), where the terms with odd powers of β contribute to the directionality, while terms of order β^2 are detrimental. This contrasts with the standard case of neglecting field propagation, where $\beta < 1$ does not change the qualitative behavior of guided emission. In the limit $\beta \ll 1$

$$\chi(\Psi_0) \approx -\mathcal{C} \sin\phi \sin\Delta\phi, \qquad (8)$$

where $\mathcal{C} = \sin 2\theta$ is the concurrence that characterizes the entanglement of a pure state $|\Psi_0\rangle$. Thus, for small waveg-

uide coupling efficiencies, the directionality χ could be a direct measure of the entanglement of the emitters. This also indicates that directional emission can be observed even in experiments with low coupling efficiency between emitters and waveguides.

We discuss the various parameter dependencies of the directionality below:

(1) Dependence on average propagation phase ($\phi = \frac{\phi_R + \phi_L}{2}$): Directionality comes from having constructive interference in one direction and destructive interference in the other direction. Considering the phases of field propagation $\phi_R = 2n\pi$ and $\phi_L = (2m+1)\pi$, gives $\phi = (n + \frac{1}{2})\pi$. We see that this maximizes the overall prefactor $\sin\phi$ and thus the directionality.

(2) Dependence on the relative atomic and field phases ($\Delta\phi$): The interference effects between the atomic dipoles and the field are represented by the $\sin\Delta\phi$ term, which maximizes directionality for $\sin\Delta\phi \to 1$. This can be clearly seen from both Figs. 3(a) and 3(b).

(3) Dependence on waveguide coupling efficiency (β) and initial atomic excitation amplitudes (θ): In the case of $\beta \to 0$, there is nearly zero probability of multiple reflections, absorptions, and reemissions of the field in the waveguide, such that the field from one atom perfectly interferes (constructive or destructively) with the field from the other atom. For $\beta \to 1$, the optimum directionality occurs when one atom radiates most of the field, while the second provides just enough field required for constructive interference [as seen from Fig. 3(a)]. This case corresponds to the optimum value $\theta = \pi/8$.

Directionality can aid in sensing either the relative atomic phases or field propagation phases φ,[5] all other experimental parameters being fixed. In order to quantify this advantage we define $\mathcal{F}_D(\varphi) \equiv \sum_{i=L,R,\text{out}} P_i[\partial \log(P_i)/\partial\varphi]^2$ as the Fisher information that considers directionality. Here P_i is the probability of emission into the decay channel i, spanning over modes propagating to the left (P_L), right (P_R), and out of the waveguide [$P_{\text{out}} = 1 - (P_R + P_L)$]. To compare with the case where one ignores directionality, we define the nondirectional Fisher information $\mathcal{F}_{\text{ND}}(\varphi) \equiv \sum_{i=\text{tot,out}} P_i[\partial \log(P_i)/\partial\varphi]^2$, that considers only the total decay into and outside the waveguide with probabilities P_{tot} and P_{out}, respectively. It can be shown that $\mathcal{F}_D(\varphi) \geqslant \mathcal{F}_{\text{ND}}(\varphi)$ (see Appendix D), meaning that distinguishing the direction of propagation of the emitted photon helps to better estimate the general phase φ.

V. EXTENSION TO N ATOMS

Having illustrated the key features of the dynamics in the presence of anisotachy, we now consider an extension of the system to the case of N atoms, as shown in Fig. 4. We consider an array of N atoms, each separated from its nearest neighbor by a distance d and connected via an asymmetric waveguide configuration that allows for anisotachy.

Assuming an initial state of the total system to have only one excitation, the subsequent state of the system can be
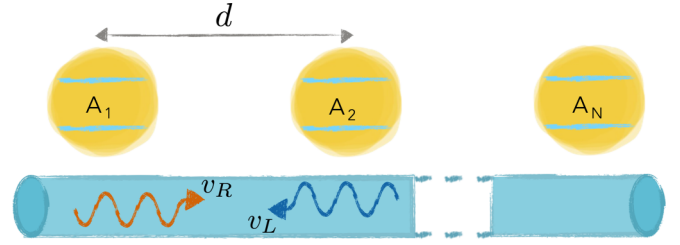
---

[5]Here φ could refer to either the atomic phases [ϕ_{A_1}, ϕ_{A_2}], the field propagation phases [ϕ_R, ϕ_L], or the relative phases [$\Delta\phi, \phi$].

FIG. 4. Schematic representation of N atoms coupled to a waveguide in an configuration with anisotachy.

written as

$$|\Psi(t)\rangle = \left\{ \sum_{m=1}^{N} c_m(t)\hat{\sigma}_m^+ + \int_0^\infty [c_R(\omega, t)\hat{a}_R^\dagger(\omega) + c_L(\omega, t)]\hat{a}_L^\dagger \right\} |gg\ldots g\rangle \otimes |[0]\rangle. \quad (9)$$

For atoms placed in a one-dimensional regular array, the equations of motion for the atomic excitation amplitudes, after eliminating the field modes, can be written as

$$\dot{c}_m(t) = -\frac{\gamma}{2}\left\{ c_m(t) + \beta\left[\sum_{n<m} e^{i(m-n)\phi_R} c_n\left(t - (m-n)\frac{d}{v_R}\right) + \sum_{n>m} e^{i(n-m)\phi_L} c_n\left(t - (n-m)\frac{d}{v_L}\right) \right] \right\}. \quad (10)$$

As in the previous section, we focus on the limit of small atomic separation ($\gamma T \ll 1$), and consider the resulting collective atomic dynamics. The above set of coupled delay differential equations can be thus solved to obtain the dynamics of the N-atom system. Considering the column vector $\overrightarrow{C}(t)$ with entries $c_m(t)$, we can write the system of equations as

$$\dot{\overrightarrow{C}}(t) = -\frac{\gamma}{2}[\overset{\leftrightarrow}{\mathcal{I}} + \beta(\overset{\leftrightarrow}{\mathbf{R}} + \overset{\leftrightarrow}{\mathbf{L}})]\overrightarrow{C}(t), \quad (11)$$

where $\overset{\leftrightarrow}{\mathcal{I}}$ is the $N \times N$ identity matrix and $\overset{\leftrightarrow}{\mathbf{R}}$ ($\overset{\leftrightarrow}{\mathbf{L}}$) is a strictly lower (upper) triangular matrix with nonzero elements given by $R_{nm} = e^{i(m-n)\phi_R}$ ($L_{nm} = e^{i(n-m)\phi_L}$). The dynamics of the system can then be solved as an eigenvalues problem [45], where the largest (smaller) eigenvalue corresponds to the decay rate of the most superradiant (subradiant) state. Through numerical exploration, we find that the eigenvalue corresponding to the most superradiant state increases linearly with the number of emitters. On the other hand, the eigenvalue corresponding to the most subradiant state decreases polynomially as N^{-3}, except when all the propagation phases are integer multiples of 2π leading to an eigenvalue zero regardless of the number of emitters. These results reproduce the expected behavior for a one-dimensional chain of atoms [15]. In this sense, anisotachy does not change the overall scaling of collective behavior but instead modifies the evolution at the level of the individual emitters.
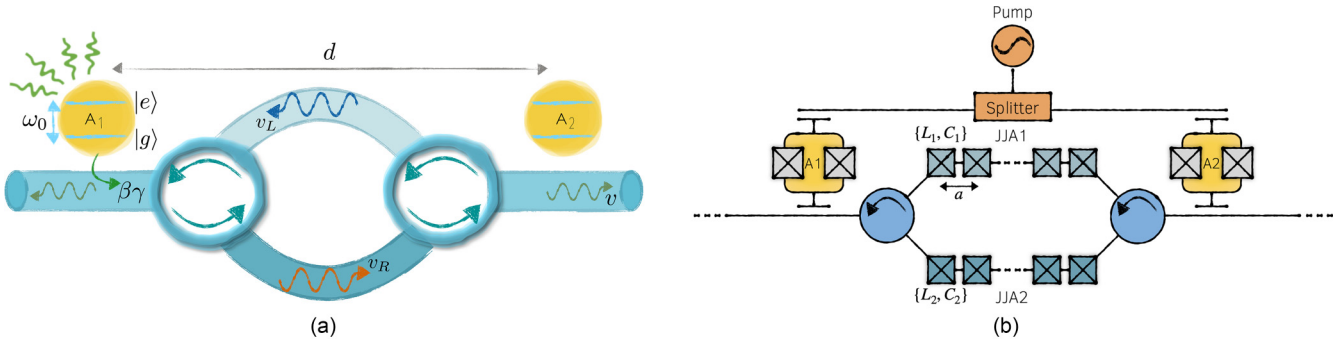
FIG. 5. (a) Schematic representation for realization of anisotachy with circulators. The atoms are connected to a waveguide, which in turn connects to circulators that are coupled to two separate waveguides with different field velocities, such that the left (right) propagating modes have a velocity v_L (v_R). The velocity of the field in the waveguide outside of the circulator region is v_o. (b) Schematic representation of a circuit QED implementation of the model. Two transmons (A1 and A2) coupled via circulators and Josephson junction (JJ) arrays (JJA1 and JJA2). The transmons are also coupled to each other via a control line that can allow for entangled state preparation by driving the qubits with an external pump field.

VI. IMPLEMENTATION IN A CIRCUIT QED SYSTEM

The proposed system can be implemented with field circulators, that are readily available for fiber optics and an active element of research in superconducting circuits [46,47] and integrated photonics [48,49]. These can be integrated into state-of-the art waveguide QED platforms [50].

We discuss a possible implementation of the present model in a circuit QED platform, as shown in Fig. 5. One can consider a system of two transmons coupled via two separate Josephson junction arrays (JJAs), that allow for low-loss propagation of microwave fields with slow velocities [51]. We assume some typical parameter values for the proposed system as shown in Table II.

The JJ arrays are considered to be made of $N \approx 2000$ junctions, and in the regime of relevant frequencies each junction can be modeled as a linear LC oscillator, with inductance $L_{1(2)}$ and capacitance $C_{1(2)}$, capacitively coupled to the ground with a ground capacitance C_g. The inductance and capacitance values are assumed to be: $L_1 \approx 1$ nH, $L_2 \approx 1.58$ nH, $C_1 \approx C_2 \approx 1$ fF, $C_g \approx 100$ fF [51–53]. The size of the unit cell in the JJ array is assumed to be $a = 10 \, \mu$m. With the above set of parameters, and a distance $d \approx 1.6$ cm (such that $\gamma d/v \approx 1$) between the emitters one can realize the parameter values considered.

VII. SUMMARY AND OUTLOOK

We have proposed a system composed of two distant emitters coupled via a waveguide where the guided field expe-

riences a direction-dependent propagation velocity. We show that in such a system the collective decay of the emitters can be nonsimultaneous and, with an appropriate set of parameters, while one of the atoms can exhibit enhanced radiative decay the other one is inhibited [Fig. 2(a)]. This suggests that collective decay can be described by local atom-photon interference processes that lead to a mutually stimulated emission of the atoms [Eq. (4)]. The power radiated by such a pair of emitters can have a high directionality controlled by their phase relation and field propagation phase [Fig. 2(b)]. Such directional emission is a rather general feature of collective delocalized systems [Eq. (6)]. We analyze the directionality of emission as a function of various parameters, characterizing the optimal conditions for directional emission (Fig. 3). Our results suggest that such directional emission can also be observed for waveguides with low coupling efficiencies. We further remark that the dynamics of the emitters described here shares commonalities with classical systems [54]. Nonetheless, in the proposed model, the directionallity of the coupling aids the detection of entanglement [Eq. (8)] and helps distinguish between the symmetric and asymmetric entangled states of two emitters (Fig. 3). We finally propose a possible implementation of the scheme in a superconducting circuit platform in Sec. VI.

While on the one hand our results show that directional emission could be used for state tomography and measuring entanglement, on the other hand one can prepare the emitters in an entangled state by driving them through the waveguide. This can be thought as the time reversal process of collective directional emission [39,55,56]. The directional emission and state preparation protocols can allow for efficient and controllable routing of quantum information in quantum networks [31,32,57,58].

The phenomena described in this work can be extended to study directional emission from collective many-body quantum states, with the presented system as a fundamental unit along a chain of emitters coupled to an *anisotachyic* bath. Additionally, for strongly driven systems, the effects of atomic nonlinearity become relevant [59,60]. It has been shown, for example, that nonlinearity can assist

TABLE II. Parameter values for a superconducting circuit implementation of the model as depicted in Fig. 5.

Qubit resonance frequency $\omega_0/(2\pi)$	5 GHz
Decay rate $\gamma/(2\pi)$	10 MHz
Waveguide coupling efficiency β	0.95
Phase velocity in JJA1 v_1/c	0.0033
Phase velocity in JJA2 v_2/c	0.0026

in directional emission [31,61–63]. It would therefore be pertinent to analyze and optimize the directionality over a broader set of parameters including general atomic states, field propagation phases in nonlinear systems and anisotachy.

Anisotachy in waveguide QED platforms could offer new ways to manipulate light-matter interactions. In particular, we show here that it can be used to couple delocalized correlated state of two emitters to a specific direction of collective radiation. This effect expands the toolbox for quantum optics applications while enriching our understanding of waveguide QED systems.

APPENDIX A: DERIVATION OF THE EQUATIONS OF MOTION

We can write the coupled emitter-field equations of motion from Eqs. (2) and (4) as

$$\dot{c}_{\mathrm{R}}(\omega, t) = -i \sum_{m=1,2} c_m(t)[g(\omega)]^* e^{-i\omega x_m/v_{\mathrm{R}}} e^{i(\omega-\omega_0)t}, \tag{A1}$$

$$\dot{c}_{\mathrm{L}}(\omega, t) = -i \sum_{m=1,2} c_m(t)[g(\omega)]^* e^{i\omega x_m/v_{\mathrm{L}}} e^{i(\omega-\omega_0)t}, \tag{A2}$$

$$\dot{c}_m(t) = -i \int_0^\infty d\omega\, g(\omega) e^{-i(\omega-\omega_0)t} \left[c_{\mathrm{R}}(\omega, t) e^{i\omega x_m/v_{\mathrm{R}}} + c_{\mathrm{L}}(\omega, t) e^{-i\omega x_m/v_{\mathrm{L}}} \right]. \tag{A3}$$

Formal integration of (A1) and (A2) yields

$$c_{\mathrm{R}}(\omega, t) = -i \int_0^t d\tau \sum_{m=1,2} g^*(\omega) c_m(\tau) e^{-i\omega x_m/v_{\mathrm{R}}} e^{i(\omega-\omega_0)\tau}, \tag{A4}$$

$$c_{\mathrm{L}}(\omega, t) = -i \int_0^t d\tau \sum_{m=1,2} g^*(\omega) c_m(\tau) e^{i\omega x_m/v_{\mathrm{L}}} e^{i(\omega-\omega_0)\tau}. \tag{A5}$$

Substituting the above in Eq. (A3), we can rewrite the atomic equation as follows:

$$\dot{c}_m(t) = -\int_0^\infty d\omega\, |g(\omega)|^2 \int_0^t d\tau \sum_{n=1,2} c_n(\tau) e^{-i(\omega-\omega_0)(t-\tau)} \left(e^{i\omega(x_m-x_n)/v_{\mathrm{R}}} + e^{-i\omega(x_m-x_n)/v_{\mathrm{L}}} \right). \tag{A6}$$

We now define the field correlation function $F(s) = \int_0^\infty d\omega |g(\omega)|^2 e^{-i(\omega-\omega_0)s}$, to obtain

$$\dot{c}_m(t) = -\int_0^t d\tau \left\{ 2c_m(\tau) F(t-\tau) + c_n(\tau) \left[e^{i\omega_0 T_{\mathrm{R}}^{mn}} F\left(t-\tau-T_{\mathrm{R}}^{mn}\right) + e^{-i\omega_0 T_{\mathrm{L}}^{mn}} F\left(t-\tau+T_{\mathrm{L}}^{mn}\right) \right] \right\}, \tag{A7}$$

where $T_{\mathrm{R,L}}^{mn} = (x_m - x_n)/v_{\mathrm{R,L}}$ is the direction dependent delay time for the light propagating between the emitters.

In the standard Markov approximation $F(\tau) = 2\pi |g(\omega_0)|^2 \delta(\tau)$, though more generally $F(\tau)$ is a narrow distribution symmetric around $s = 0$. We assume that the temporal width σ of such distribution is narrower than the delay time between the emitters $(\sigma < |T_{L,R}^{mn}|)$,

$$\dot{c}_m(t) = -2 \int_0^t d\tau\, c_m(t-\tau) F(\tau) - e^{i\omega_0 T^{mn}} \int_{-T^{mn}}^{t-T^{mn}} d\tau\, c_n(t-\tau-T^{mn}) F(\tau), \tag{A8}$$

where $T^{12} = T_{\mathrm{L}}^{12} = T_{\mathrm{L}}$ or $T^{21} = T_{\mathrm{R}}^{21} = T_{\mathrm{R}}$. If σ is small enough we can assume that the amplitude of the coefficients does not vary significantly over the region where $F(\tau)$ is nonzero, such that $c_m(t-\tau) \approx c_m(t)$. Thus given that $F(\tau)$ is symmetric, centered around $\tau = 0$ and narrower than T^{mn} we have

$$\dot{c}_m(t) \approx -2c_m(t) \int_0^\infty ds\, F(s) - c_n(t-T^{mn})\Theta(t-T^{mn}) e^{i\omega_0 T^{mn}} \int_{-\infty}^\infty d\tau\, F(\tau). \tag{A9}$$

The term $F(\tau)$ is a complex function with the real and imaginary part being even and odd functions respectively. We define

$$\frac{\gamma}{2} = 2\mathrm{Re}\left[\int_0^\infty d\tau\, F(\tau) \right] = \mathrm{Re}\left[\int_{-\infty}^\infty d\tau\, F(\tau) \right], \tag{A10}$$

$$\Delta_L = \mathrm{Im}\left[\int_0^\infty d\tau\, F(\tau) \right], \tag{A11}$$

where Δ_L is the Lamb shift, which we include as a part of the emitters renormalized resonance frequency ω_0.

Introducing a phenomenological cross-coupling efficiency β between the emitters $(0 \leqslant \beta \leqslant 1)$, one can simplify Eq. (A9) to obtain the atomic equations of motion [Eq. (4)].

APPENDIX B: ATOMIC DYNAMICS

1. Lambert W-function solution

Taking the Laplace transform of Eq. (4), one gets

$$s\tilde{c}_1(s) - c_1(0) = -\frac{\gamma}{2}[\tilde{c}_1(s) + \beta\tilde{c}_2(s)e^{-sT_L}e^{i\phi_L}], \tag{B1}$$

$$s\tilde{c}_2(s) - c_2(0) = -\frac{\gamma}{2}[\tilde{c}_2(s) + \beta\tilde{c}_1(s)e^{-sT_R}e^{i\phi_R}], \tag{B2}$$

which can be solved to obtain the Laplace coefficients pertaining to the two emitters as follows:

$$\tilde{c}_1(s) = \frac{c_1(0)\left(s + \frac{\gamma}{2}\right) - c_2(0)\beta\frac{\gamma}{2}e^{-sT_L}e^{i\phi_L}}{\left(s + \frac{\gamma}{2}\right)^2 - \left(\beta\frac{\gamma}{2}e^{-sT}e^{i\phi}\right)^2}, \tag{B3}$$

$$\tilde{c}_2(s) = \frac{c_2(0)\left(s + \frac{\gamma}{2}\right) - c_1(0)\beta\frac{\gamma}{2}e^{-sT_R}e^{i\phi_R}}{\left(s + \frac{\gamma}{2}\right)^2 - \left(\beta\frac{\gamma}{2}e^{-sT}e^{i\phi}\right)^2}. \tag{B4}$$

The poles of the above Laplace coefficients are given by

$$s_n^{\pm} = -\frac{\gamma}{2} + \frac{1}{T}W_n\left(\mp\beta\frac{\gamma T}{2}e^{\gamma T/2}e^{i\phi}\right), \tag{B5}$$

where W_n is the nth branch of the Lambert W-function [64].

We can thus rewrite the Eqs. (B3) and (B4) as

$$\tilde{c}_m(s) = \sum_{\pm}\sum_{n=-\infty}^{\infty}\frac{\alpha_{n,m}^{\pm}}{s - s_n^{\pm}}, \tag{B6}$$

where the coefficients $\alpha_{n,m}^{\pm}$ are obtained as

$$\alpha_{n,m}^{\pm} = \lim_{s\to s_n^{\pm}}\tilde{c}_m(s)(s - s_n^{\pm}). \tag{B7}$$

Thus taking the inverse Laplace transform of Eq. (B6), we get

$$c_m(t) = \sum_{\sigma=+,-}\sum_{n=-\infty}^{\infty}\alpha_{n,m}^{\sigma}e^{-\gamma_n^{\sigma}t}, \tag{B8}$$

where

$$\gamma_n^{\pm} = \frac{\gamma}{2} - \frac{1}{T}W_n\left(\mp\frac{\beta\gamma T}{2}e^{\gamma T/2}e^{i\phi}\right), \tag{B9}$$

$$\alpha_{n,1}^{\pm} = \frac{1}{2}\frac{c_1(0) \pm c_2(0)e^{i(\phi_L-\phi_R)/2}e^{(T_L-T_R)\gamma_n^{\pm}/2}}{1 + W_n\left(\mp\frac{\beta\gamma T}{2}e^{\gamma T/2}e^{i\phi}\right)}, \tag{B10}$$

$$\alpha_{n,2}^{\pm} = \frac{1}{2}\frac{c_2(0) \pm c_1(0)e^{-i(\phi_L-\phi_R)/2}e^{-(T_L-T_R)\gamma_n^{\pm}/2}}{1 + W_n\left(\mp\frac{\beta\gamma T}{2}e^{\gamma T/2}e^{i\phi}\right)}. \tag{B11}$$

2. Series expansion solution

An alternative way of expressing the atomic excitation amplitudes as the inverse Laplace transform of Eqs. (B3) and (B4) in terms of a series solution is as follows [42]:

$$c_1(t) = \frac{1}{2\pi i}\lim_{\epsilon\to 0}\int_{-i\infty+\epsilon}^{+i\infty+\epsilon}ds\frac{c_1(0)\left(s + \frac{\gamma}{2}\right) - c_2(0)\frac{\beta\gamma}{2}e^{-sT_L}e^{i\phi_L}}{\left(s + \frac{\gamma}{2}\right)^2}\left[\sum_{n=0}^{\infty}\left(\frac{\beta\gamma/2e^{-sT}e^{i\phi}}{s+\gamma/2}\right)^{2n}\right], \tag{B12}$$

$$= c_1(0)\underbrace{\frac{1}{2\pi i}\int ds\left\{\frac{1}{s+\gamma/2}\left[\sum_{n=0}^{\infty}\left(\frac{\beta\gamma/2e^{-sT}e^{i\phi}}{s+\gamma/2}\right)^{2n}\right]\right\}}_{\text{(Ia)}} - c_2(0)\underbrace{\frac{1}{2\pi i}\int ds\left\{\frac{\beta\gamma}{2}\frac{e^{-sT_L}e^{i\phi_L}}{(s+\gamma/2)^2}\left[\sum_{n=0}^{\infty}\left(\frac{\beta\gamma/2e^{-sT}e^{i\phi}}{s+\gamma/2}\right)^{2n}\right]\right\}}_{\text{(IIa)}}. \tag{B13}$$

$$c_2(t) = \frac{1}{2\pi i} \lim_{\epsilon \to 0} \int_{-i\infty+\epsilon}^{+i\infty+\epsilon} ds \frac{c_2(0)\left(s+\frac{\gamma}{2}\right) - c_1(0)\frac{\beta\gamma}{2}e^{-sT_R}e^{i\phi_R}}{\left(s+\frac{\gamma}{2}\right)^2} \left[\sum_{n=0}^{\infty} \left(\frac{\beta\gamma/2e^{-sT}e^{i\phi}}{s+\gamma/2}\right)^{2n}\right],$$
(B14)

$$= c_2(0) \underbrace{\frac{1}{2\pi i}\int ds \left\{\frac{1}{s+\gamma/2}\left[\sum_{n=0}^{\infty}\left(\frac{\beta\gamma/2e^{-sT}e^{i\phi}}{s+\gamma/2}\right)^{2n}\right]\right\}}_{\text{(Ib)}} - c_1(0) \underbrace{\frac{1}{2\pi i}\int ds \left\{\frac{\beta\gamma}{2}\frac{e^{-sT_R}e^{i\phi_R}}{(s+\gamma/2)^2}\left[\sum_{n=0}^{\infty}\left(\frac{\beta\gamma/2e^{-sT}e^{i\phi}}{s+\gamma/2}\right)^{2n}\right]\right\}}_{\text{(IIb)}}.$$
(B15)

We identify the terms (Ia) = (Ib) ≡ (I) as corresponding to the round trip times (even number) of the field between the atoms and the terms (IIa) and (IIb) (not necessarily equal to each other) as the terms coming from odd number of trips between the atoms. Simplifying each of the above terms:

$$\text{(I)} = \frac{1}{2\pi i}\int ds \left\{\frac{1}{s+\gamma/2}\left[\sum_{n=0}^{\infty}\left(\frac{\beta\gamma/2e^{-sT}e^{i\phi}}{s+\gamma/2}\right)^{2n}\right]\right\},$$
(B16)

$$= \sum_n \frac{(\beta\gamma e^{i\phi}/2)^{2n}}{(2n)!}(t-2nT)^{2n}e^{-\gamma/2(t-2nT)}\Theta(t-2nT),$$
(B17)

$$\text{(IIa)} = \frac{1}{2\pi i}\int ds \left\{\frac{\beta\gamma}{2}\frac{e^{-sT_L}e^{i\phi_L}}{(s+\gamma/2)^2}\left[\sum_{n=0}^{\infty}\left(\frac{\beta\gamma/2e^{-sT}e^{i\phi}}{s+\gamma/2}\right)^{2n}\right]\right\},$$
(B18)

$$= \sum_n \frac{(\beta\gamma/2)^{2n+1}}{(2n+1)!}e^{i2n\phi+i\phi_L}(t-2nT-T_L)^{2n+1}e^{-\gamma/2(t-2nT-T_L)}\Theta(t-2nT-T_L),$$
(B19)

$$\text{(IIb)} = \frac{1}{2\pi i}\int ds \left\{\frac{\beta\gamma}{2}\frac{e^{-sT_R}e^{i\phi_R}}{(s+\gamma/2)^2}\left[\sum_{n=0}^{\infty}\left(\frac{\beta\gamma/2e^{-sT}e^{i\phi}}{s+\gamma/2}\right)^{2n}\right]\right\},$$
(B20)

$$= \sum_n \frac{(\beta\gamma/2)^{2n+1}}{(2n+1)!}e^{i2n\phi+i\phi_R}(t-2nT-T_R)^{2n+1}e^{-\gamma/2(t-2nT-T_R)}\Theta(t-2nT-T_R).$$
(B21)

We substitute the above in Eqs. (B13) and (B15) to obtain the dynamics of general initial states given by Eq. (4).

We plot the atomic dynamics as a function of time in Fig. 6. It can be seen that when the sign of the atomic coefficients $c_{1,2}$ changes, so does the sign of its electric dipole moment that drives the field, causing the atoms to switch from absorbing to emitting, or vice versa.

APPENDIX C: INTENSITY DYNAMICS

The intensity of the field emitted by the atoms as a function of position and time can be evaluated as $I(x,t) = \frac{\epsilon_0 c}{2}\langle\Psi(t)|\hat{E}^\dagger(x,t)\hat{E}(x,t)|\Psi(t)\rangle$, where $\hat{E}(x,t) = \int_0^\infty d\omega\, \mathcal{E}_\omega[\hat{a}_L(\omega)e^{-ik_L x} + \hat{a}_R(\omega)e^{ik_R x}]e^{-i\omega t}$ is the electric field operator at position x and time t. More explicitly, we obtain

$$I(x,t) = \frac{\epsilon_0 c|\mathcal{E}_0|^2}{2}\langle\Psi(t)|\left\{\int d\omega_1[\hat{a}_L^\dagger(\omega_1)e^{ik_{1L}x} + \hat{a}_R^\dagger(\omega_1)e^{-ik_{1R}x}]e^{i\omega_1 t}\int d\omega_2[\hat{a}_L(\omega_2)e^{-ik_{2L}x} + \hat{a}_R(\omega_2)e^{ik_{2R}x}]e^{-i\omega_2 t}\right\}|\Psi(t)\rangle,$$
(C1)

$$= \frac{\epsilon_0 c|\mathcal{E}_0|^2}{2}\langle\Psi(t)|\int d\omega_1 \int d\omega_2[e^{i(k_{1L}-k_{2L})x}c_L^*(\omega_1,t)c_L(\omega_2,t) + e^{-i(k_{1R}-k_{2R})x}c_R^*(\omega_1,t)c_R(\omega_2,t)$$
$$+ e^{-i(k_{1R}+k_{2L})x}c_R^*(\omega_1,t)c_L(\omega_2,t) + e^{i(k_{1L}+k_{2R})x}c_L^*(\omega_1,t)c_R(\omega_2,t)]e^{i(\omega_1-\omega_2)t}|\Psi(t)\rangle,$$
(C2)

$$= \frac{\epsilon_0 c|\mathcal{E}_0|^2}{2}\langle\Psi(t)|\left|\int d\omega[c_L(\omega,t)e^{-i\omega x/v_L} + c_R(\omega,t)e^{i\omega x/v_R}]e^{-i\omega t}\right|^2|\Psi(t)\rangle,$$
(C3)

$$= \frac{\epsilon_0 c|\mathcal{E}_0|^2\gamma\beta}{4\pi}\left|\int d\omega e^{-i\omega t}\left\{\int_0^t d\tau[c_1(\tau)e^{i\omega(-x+x_1)/v_L} + c_2(\tau)e^{i\omega(-x+x_2)/v_L}\right.\right.$$
$$\left.\left. + c_1(\tau)e^{-i\omega(-x+x_1)/v_R} + c_2(\tau)e^{-i\omega(-x+x_2)/v_R}]e^{i(\omega-\omega_0)\tau}\right\}\right|^2,$$
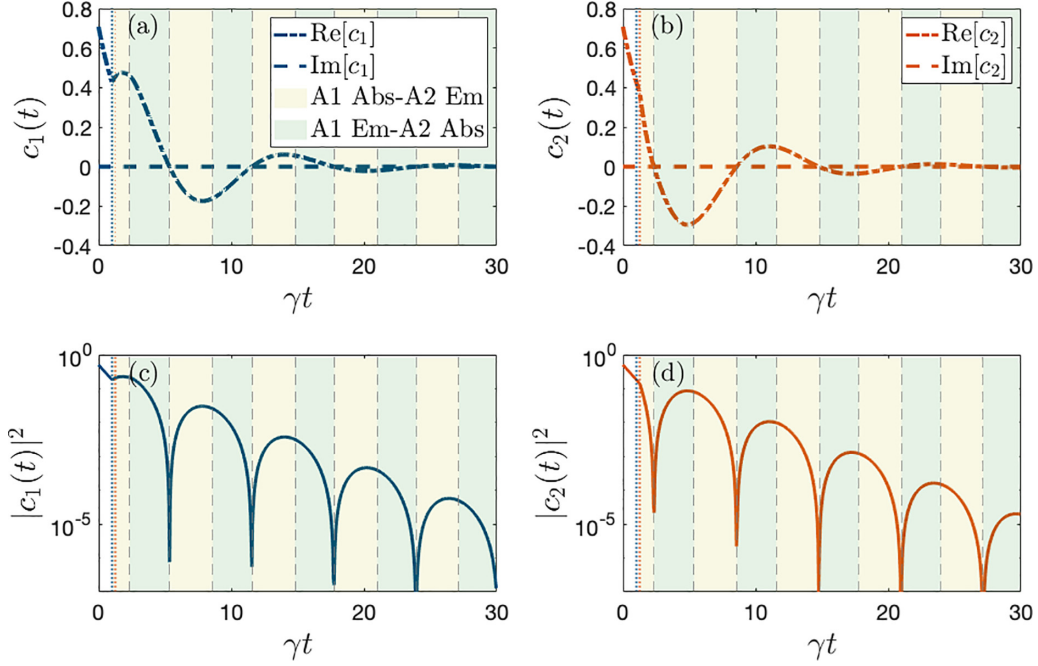(C4)

FIG. 6. Dynamics of atomic coefficients (a) $c_1(t)$ and (b) $c_2(t)$, and atomic populations (c) $|c_1(t)|^2$ and (d) $|c_2(t)|^2$. Whenever the atomic coefficients change sign ($c_{1,2}(t) = 0$) the atomic populations reverse their absorption and emission behavior, as indicated by the yellow and green regions corresponding to atom A1 absorbing-A2 emitting and A1 emitting-A2 absorbing, respectively.

where we have used Eqs. (A1) and (A2) to substitute the field amplitudes in terms of the atomic excitation amplitudes. Using the W-function solution for the atomic coefficients [Eq. (B8)] and performing the integrals over time and frequency, we obtain

$$
\begin{aligned}
I/I_0 = \Bigg| &\sum_{\sigma=+,-} \sum_{n=-\infty}^{\infty} \big(\alpha_{n,1}^{\sigma} e^{-i(\omega_0 - i\gamma_n^{\sigma})[t+(x-x_1)/v_L]} \{\Theta[t+(x-x_1)/v_L] - \Theta[(x-x_1)/v_L]\} \\
&+ \alpha_{n,2}^{\sigma} e^{-i(\omega_0 - i\gamma_n^{\sigma})[t+(x-x_2)/v_L]} \{\Theta[t+(x-x_2)/v_L] - \Theta[(x-x_2)/v_L]\} \\
&+ \alpha_{n,1}^{\sigma} e^{-i(\omega_0 - i\gamma_n^{\sigma})[t-(x-x_1)/v_R]} \{\Theta[t-(x-x_1)/v_R] - \Theta[-(x-x_1)/v_R]\} \\
&+ \alpha_{n,2}^{\sigma} e^{-i(\omega_0 - i\gamma_n^{\sigma})[t-(x-x_2)/v_R]} \{\Theta[t-(x-x_2)/v_R] - \Theta[-(x-x_2)/v_R]\} \big) \Bigg|^2 .
\end{aligned}
\tag{C5}
$$

We can rewrite the above in terms of the atomic excitation amplitudes using Eq. (B8) as

$$
\begin{aligned}
I/I_0 = \Big| &\big(c_1[t+(x+d/2)/v_L] e^{-i\omega_0(x+d/2)/v_L} \{\Theta[t+(x+d/2)/v_L] - \Theta[(x+d/2)/v_L]\} \\
&+ c_2[t+(x-d/2)/v_L] e^{-i\omega_0(x-d/2)/v_L} \{\Theta[t+(x-d/2)/v_L] - \Theta[(x-d/2)/v_L]\} \\
&+ c_1[t-(x+d/2)/v_R] e^{i\omega_0(x+d/2)/v_R} \{\Theta[t-(x+d/2)/v_R] - \Theta[-(x+d/2)/v_R]\} \\
&+ c_2[t-(x-d/2)/v_R] e^{i\omega_0(x-d/2)/v_R} \{\Theta[t-(x-d/2)/v_R] - \Theta[-(x-d/2)/v_R]\} \big) \Big|^2,
\end{aligned}
\tag{C6}
$$

which corresponds to Eq. (6).

APPENDIX D: DIRECTIONAL EMISSION

Let us consider the dynamics for the atomic coefficients given by Eq. (5). In the limit $\gamma T \ll 1$, neglecting the delay but keeping the propagation phases, we obtain

$$
c_1(t) = \left[c_1(0) \sum_{n=0}^{\infty} \frac{\left(\beta \frac{\gamma}{2} t e^{i\phi}\right)^{2n}}{2n!} - c_2(0) e^{i(\phi_L - \phi)} \sum_{n=0}^{\infty} \frac{\left(\beta \frac{\gamma}{2} t e^{i\phi}\right)^{2n+1}}{(2n+1)!} \right] e^{-\frac{\gamma}{2}t} \Theta(t),
\tag{D1}
$$

$$c_2(t) = \left[c_2(0) \sum_{n=0}^{\infty} \frac{\left(\beta \frac{\gamma}{2} t e^{i\phi}\right)^{2n}}{2n!} - c_1(0) e^{i(\phi_R - \phi)} \sum_{n=0}^{\infty} \frac{\left(\beta \frac{\gamma}{2} t e^{i\phi}\right)^{2n+1}}{(2n+1)!} \right] e^{-\frac{\gamma}{2} t} \Theta(t). \tag{D2}$$

These series converges to

$$c_1(t) = \left[c_1(0) \cosh\left(\beta \frac{\gamma}{2} t e^{i\phi}\right) - c_2(0) e^{i(\phi_L - \phi)} \sinh\left(\beta \frac{\gamma}{2} t e^{i\phi}\right) \right] e^{-\frac{\gamma}{2} t} \Theta(t), \tag{D3}$$

$$c_2(t) = \left[c_2(0) \cosh\left(\beta \frac{\gamma}{2} t e^{i\phi}\right) - c_1(0) e^{i(\phi_R - \phi)} \sinh\left(\beta \frac{\gamma}{2} t e^{i\phi}\right) \right] e^{-\frac{\gamma}{2} t} \Theta(t). \tag{D4}$$

We now consider the field coefficients in the steady state ($t \to \infty$), which can be simplified to

$$c_R(\omega, t \to \infty)$$

$$= -i g^*(\omega) e^{-i\frac{\phi_R}{2}} \left\{ [c_1(0) e^{i\phi_R} + c_2(0)] \frac{\left(\frac{\gamma}{2} - i\Delta\right)}{\left(\frac{\gamma}{2} - i\Delta\right)^2 - \left(\beta \frac{\gamma}{2} e^{i\phi}\right)^2} - [c_2(0) e^{2i\phi} + c_1(0) e^{i\phi_R}] \frac{\beta \frac{\gamma}{2}}{\left(\frac{\gamma}{2} - i\Delta\right)^2 - \left(\beta \frac{\gamma}{2} e^{i\phi}\right)^2} \right\}, \tag{D5}$$

$$c_L(\omega, t \to \infty)$$

$$= -i g^*(\omega) e^{-i\frac{\phi_L}{2}} \left\{ [c_1(0) + c_2(0) e^{i\phi_L}] \frac{\left(\frac{\gamma}{2} - i\Delta\right)}{\left(\frac{\gamma}{2} - i\Delta\right)^2 - \left(\beta \frac{\gamma}{2} e^{i\phi}\right)^2} - [c_2(0) e^{i\phi_L} + c_1(0) e^{2i\phi}] \frac{\beta \frac{\gamma}{2}}{\left(\frac{\gamma}{2} - i\Delta\right)^2 - \left(\beta \frac{\gamma}{2} e^{i\phi}\right)^2} \right\}. \tag{D6}$$

The probability of emitting the photon to the right (left) is thus given by

$$P_{R(L)} = \int_0^{\infty} d\omega |c_{R(L)}(\omega, t \to \infty)|^2. \tag{D7}$$

We parametrize the initial atomic coefficients as $c_1(0) = e^{i\phi_{A1}} \cos\theta$ and $c_2(0) = e^{i\phi_{A2}} \sin\theta$, to obtain the right and left emission probabilities as follows:

$$P_R = |g(\omega_0)|^2 \int_0^{\infty} d\omega \left| (\sin\theta + \cos\theta e^{i\Delta\phi} e^{i\phi}) \frac{\left(\frac{\gamma}{2} - i\Delta\right)}{\left(\frac{\gamma}{2} - i\Delta\right)^2 - \left(\beta \frac{\gamma}{2} e^{i\phi}\right)^2} - (\sin\theta + \cos\theta e^{i\Delta\phi} e^{-i\phi}) e^{2i\phi} \frac{\beta \frac{\gamma}{2}}{\left(\frac{\gamma}{2} - i\Delta\right)^2 - \left(\beta \frac{\gamma}{2} e^{i\phi}\right)^2} \right|^2, \tag{D8}$$

$$P_L = |g(\omega_0)|^2 \int_0^{\infty} d\omega \left| (\sin\theta + \cos\theta e^{i\Delta\phi} e^{-i\phi}) \frac{\left(\frac{\gamma}{2} - i\Delta\right)}{\left(\frac{\gamma}{2} - i\Delta\right)^2 - \left(\beta \frac{\gamma}{2} e^{i\phi}\right)^2} - (\sin\theta + \cos\theta e^{i\Delta\phi} e^{i\phi}) \frac{\beta \frac{\gamma}{2}}{\left(\frac{\gamma}{2} - i\Delta\right)^2 - \left(\beta \frac{\gamma}{2} e^{i\phi}\right)^2} \right|^2. \tag{D9}$$

We consider the integral

$$I_0 = \int_0^{\infty} d\omega \left| \frac{T_1\left(\frac{\gamma}{2} - i\Delta\right) - T_2 \beta \frac{\gamma}{2}}{\left(\frac{\gamma}{2} - i\Delta\right)^2 - \left(\beta \frac{\gamma}{2} e^{i\phi}\right)^2} \right|^2, \tag{D10}$$

$$= |T_1|^2 \int_0^{\infty} d\omega \frac{\Delta^2}{\left| \left(\frac{\gamma}{2} - i\Delta\right)^2 - \left(\beta \frac{\gamma}{2} e^{i\phi}\right)^2 \right|^2} - 2 \mathrm{Im}\{T_1 T_2^*\} \beta \frac{\gamma}{2} \int_0^{\infty} d\omega \frac{\Delta}{\left| \left(\frac{\gamma}{2} - i\Delta\right)^2 - \left(\beta \frac{\gamma}{2} e^{i\phi}\right)^2 \right|^2}$$

$$+ |T_1 - T_2 \beta|^2 \left(\frac{\gamma}{2}\right)^2 \int_0^{\infty} d\omega \frac{1}{\left| \left(\frac{\gamma}{2} - i\Delta\right)^2 - \left(\beta \frac{\gamma}{2} e^{i\phi}\right)^2 \right|^2},$$

$$\equiv |T_1|^2 I_3 - 2 \mathrm{Im}\{T_1 T_2^*\} \beta \left(\frac{\gamma}{2}\right) I_2 + |T_1 - T_2 \beta|^2 \left(\frac{\gamma}{2}\right)^2 I_1, \tag{D11}$$

where we can simplify the integrals I_1, I_2, and I_3 as follows:

$$I_1 = \int_0^{\infty} d\omega \frac{1}{\left| \left(\frac{\gamma}{2} - i\Delta\right)^2 - \left(\beta \frac{\gamma}{2} e^{i\phi}\right)^2 \right|^2} = \frac{\pi}{2} \frac{1}{\left(\frac{\gamma}{2}\right)^3} \frac{1}{[1 - (\beta \cos\phi)^2][1 + (\beta \sin\phi)^2]}, \tag{D12}$$

$$I_2 = \int_0^{\infty} d\omega \frac{\Delta}{\left| \left(\frac{\gamma}{2} - i\Delta\right)^2 - \left(\beta \frac{\gamma}{2} e^{i\phi}\right)^2 \right|^2} = -\frac{\pi}{4} \frac{1}{\left(\frac{\gamma}{2}\right)^2} \frac{\beta^2 \sin 2\phi}{[1 - (\beta \cos\phi)^2][1 + (\beta \sin\phi)^2]}, \tag{D13}$$

$$I_3 = \int_0^{\infty} d\omega \frac{\Delta^2}{\left| \left(\frac{\gamma}{2} - i\Delta\right)^2 - \left(\beta \frac{\gamma}{2} e^{i\phi}\right)^2 \right|^2} = \frac{\pi}{2} \frac{1}{\left(\frac{\gamma}{2}\right)} \frac{1 - \beta^2 \cos 2\phi}{[1 - (\beta \cos\phi)^2][1 + (\beta \sin\phi)^2]}. \tag{D14}$$

Substituting the above in Eq. (D11), we get

$$I_0 = \frac{\pi}{\gamma} \frac{|T_1|^2[1 - \beta^2 \cos 2\phi] + \text{Im}(T_1 T_2^*)\beta^3 \sin 2\phi + |T_1 - T_2\beta|^2}{[1 - (\beta \cos \phi)^2][1 + (\beta \sin \phi)^2]}. \tag{D15}$$

Plugging this result back into Eq. (D9) and (D8) and considering $4\pi|g(\omega_0)|^2 = \beta\gamma$ yields

$$P_R = \frac{1}{2} \frac{\beta}{1 + (\beta \sin \phi)^2} \left\{ \frac{[1 - \beta + (\beta \sin \phi)^2](1 - \beta \cos \Delta\phi \cos \phi \sin 2\theta)}{1 - (\beta \cos \phi)^2} + \cos(\Delta\phi + \phi) \sin 2\theta + 2\beta \sin^2 \theta \sin^2 \phi \right\}, \tag{D16}$$

$$P_L = \frac{1}{2} \frac{\beta}{1 + (\beta \sin \phi)^2} \left\{ \frac{[1 - \beta + (\beta \sin \phi]^2)(1 - \beta \cos \Delta\phi \cos \phi \sin 2\theta)}{1 - (\beta \cos \phi)^2} + \cos(\Delta\phi - \phi) \sin 2\theta + 2\beta \cos^2 \theta \sin^2 \phi \right\}, \tag{D17}$$

which depends on the four parameters: β, θ, ϕ, and $\Delta\phi$. We use the above equations to obtain the total probability of emitting into the waveguide P_{tot} and the directionality parameter χ is given by Eqs. (6) and (7).

1. Optimum directionality

We give the parameter values that optimize the directionality parameter given by Eq. (6). The value of ϕ that maximizes directionality is $\phi = \frac{2n+1}{2}\pi$ such that $\sin\phi = \pm 1$. The directional parameter for the optimal value of ϕ reads

$$\chi = -\frac{\sin\Delta\phi \sin 2\theta \pm \beta \cos 2\theta}{1 + \beta^2}. \tag{D18}$$

Considering that the value of β is fixed for a given physical system, we find the global optimum over the two remaining parameters (θ, and $\Delta\phi$), yields

$$\beta \sin 2\theta \mp \cos 2\theta \sin \Delta\phi = 0$$

$$\mp \sin 2\theta \cos \Delta\phi = 0,$$

which gives the optimum values of of $\Delta\phi = (n + \frac{1}{2})\pi$ and $\theta = \pm\frac{1}{2}\arctan\frac{1}{\beta}$. This shows that the optimum value of θ in general depends on the value of β, and it tends to $\theta \to (\frac{2n+1}{2})\pi$ as $\beta \to 0$.

2. Directional Fisher information

The directional and nondirectional quantum Fisher information are defined as

$$\mathcal{F}_D(\varphi) = P_L(\varphi)\left(\frac{\partial \log P_L(\varphi)}{\partial \varphi}\right)^2 + P_R(\varphi)\left(\frac{\partial \log P_R(\varphi)}{\partial \varphi}\right)^2 + P_{\text{out}}(\varphi)\left(\frac{\partial \log P_{out}(\varphi)}{\partial \varphi}\right)^2, \tag{D19}$$

$$\mathcal{F}_{ND}(\varphi) = P_{\text{tot}}(\varphi)\left(\frac{\partial \log P_{\text{tot}}(\varphi)}{\partial \varphi}\right)^2 + P_{\text{out}}(\varphi)\left(\frac{\partial \log P_{out}(\varphi)}{\partial \varphi}\right)^2. \tag{D20}$$

The difference between the two can be found as

$$\mathcal{F}_D(\varphi) - \mathcal{F}_{ND}(\varphi) = P_L(\varphi)\left(\frac{\partial \log P_L(\varphi)}{\partial \varphi}\right)^2 + P_R(\varphi)\left(\frac{\partial \log P_R(\varphi)}{\partial \varphi}\right)^2 - P_{tot}(\varphi)\left(\frac{\partial \log P_{tot}(\varphi)}{\partial \varphi}\right)^2 \tag{D21}$$

$$= P_L(\varphi)\left(\frac{\partial P_L(\varphi)}{\partial \varphi}\frac{1}{P_L(\varphi)}\right)^2 + P_R(\varphi)\left(\frac{\partial P_R(\varphi)}{\partial \varphi}\frac{1}{P_R(\varphi)}\right)^2 - P_{tot}(\varphi)\left(\frac{\partial P_{tot}(\varphi)}{\partial \varphi}\frac{1}{P_{tot}(\varphi)}\right)^2 \tag{D22}$$

$$= \frac{1}{P_L(\varphi) + P_R(\varphi)}\left[\left(\frac{P_R(\varphi)}{P_L(\varphi)}\right)\left(\frac{\partial P_L(\varphi)}{\partial \varphi}\right)^2 + \left(\frac{P_L(\varphi)}{P_R(\varphi)}\right)\left(\frac{\partial P_R(\varphi)}{\partial \varphi}\right)^2 - 2\frac{\partial P_L(\varphi)}{\partial \varphi}\frac{\partial P_R(\varphi)}{\partial \varphi}\right] \tag{D23}$$

$$= \frac{1}{P_{tot}(\varphi)}\left[\left(\sqrt{\frac{P_R(\varphi)}{P_L(\varphi)}}\right)\left(\frac{\partial P_L(\varphi)}{\partial \varphi}\right) - \sqrt{\frac{P_L(\varphi)}{P_R(\varphi)}}\left(\frac{\partial P_R(\varphi)}{\partial \varphi}\right)\right]^2. \tag{D24}$$

Since all the probabilities are positive real numbers, this term is always positive, thus yielding

$$\mathcal{F}_D(\varphi) - \mathcal{F}_{ND}(\varphi) \geqslant 0. \tag{D25}$$

The equality is satisfied when $P_R = P_L$, corresponding to equal emission probabilities in the left and right directions.

[1] P. Meystre, *Quantum Optics: Taming the Quantum* (Springer International Publishing, Cham, 2021)

[2] A. Predojević and M. W. Mitchell, *Engineering the Atom-Photon Interaction* (Springer International Publishing, New York, 2015).

[3] J. P. Dowling and G. J. Milburn, Philos. Trans. Royal Soc. A **361**, 1655 (2003).

[4] S. Haroche and J. M. Raimond, *Exploring the Quantum* (Oxford University Press, Oxford, 2006).

[5] P. Lodahl, S. Mahmoodian, S. Stobbe, A. Rauschenbeutel, P. Schneeweiss, J. Volz, H. Pichler, and P. Zoller, Nature (London) **541**, 473 (2017).

[6] J. D. Hood, A. Goban, A. Asenjo-Garcia, M. Lu, S.-P. Yu, D. E. Chang, and H. J. Kimble, Proc. Natl. Acad. Sci. U. S. A. **113**, 10507 (2016).

[7] Y. Liu and A. A. Houck, Nat. Phys. **13**, 48 (2017).

[8] J. G. Pedersen, S. Xiao, and N. A. Mortensen, Phys. Rev. B **78**, 153101 (2008).

[9] V. S. Asadchy, M. S. Mirmoosa, A. Díaz-Rubio, S. Fan, and S. A. Tretyakov, Proc. IEEE **108**, 1684 (2020).

[10] D. Jalas, A. Petrov, M. Eich, W. Freude, S. Fan, Z. Yu, R. Baets, M. Popović, A. Melloni, J. D. Joannopoulos *et al.*, Nat. Photonics **7**, 579 (2013).

[11] M. Gross and S. Haroche, Phys. Rep. **93**, 301 (1982).

[12] R. H. Dicke, Phys. Rev. **93**, 99 (1954).

[13] N. E. Rehler and J. H. Eberly, Phys. Rev. A **3**, 1735 (1971).

[14] J. H. Eberly, Am. J. Phys. **40**, 1374 (1972).

[15] A. Asenjo-Garcia, M. Moreno-Cardoner, A. Albrecht, H. J. Kimble, and D. E. Chang, Phys. Rev. X **7**, 031024 (2017).

[16] J. A. Needham, I. Lesanovsky, and B. Olmos, New J. Phys. **21**, 073061 (2019).

[17] N. Skribanowitz, I. P. Herman, J. C. MacGillivray, and M. S. Feld, Phys. Rev. Lett. **30**, 309 (1973).

[18] D. Pavolini, A. Crubellier, P. Pillet, L. Cabaret, and S. Liberman, Phys. Rev. Lett. **54**, 1917 (1985).

[19] M. Gross, C. Fabre, P. Pillet, and S. Haroche, Phys. Rev. Lett. **36**, 1035 (1976).

[20] R. G. DeVoe and R. G. Brewer, Phys. Rev. Lett. **76**, 2049 (1996).

[21] M. Scheibner, T. Schmidt, L. Worschech, A. Forchel, G. Bacher, T. Passow, and D. Hommel, Nat. Phys. **3**, 106 (2007).

[22] R. Röhlsberger, K. Schlage1, B. Sahoo, S. Couet, and R. Rüffer, Science **328**, 1248 (2010).

[23] J. A. Mlynek, A. A. Abdumalikov, C. Eichler, and A. Wallraff, Nat. Commun. **5**, 5186 (2014).

[24] A. Goban, C.-L. Hung, J. D. Hood, S.-P. Yu, J. A. Muniz, O. Painter, and H. J. Kimble, Phys. Rev. Lett. **115**, 063601 (2015).

[25] W. Guerin, M. O. Araújo, and R. Kaiser, Phys. Rev. Lett. **116**, 083601 (2016).

[26] C. Bradac, M. T. Johnsson, M. van Breugel, B. Q. Baragiola, R. Martin, M. L. Juan, G. K. Brennen, and T. Volz, Nat. Commun. **8**, 1205 (2017).

[27] P. Solano, P. Barberis-Blostein, F. K. Fatemi, L. A. Orozco, and S. L. Rolston, Nat. Commun. **8**, 1857 (2017).

[28] Z. Wang, H. Li, W. Feng, X. Song, C. Song, W. Liu, Q. Guo, X. Zhang, H. Dong, D. Zheng, H. Wang, and D.-W. Wang, Phys. Rev. Lett. **124**, 013601 (2020).

[29] G. Ferioli, A. Glicenstein, L. Henriet, I. Ferrier-Barbut, and A. Browaeys, Phys. Rev. X **11**, 021031 (2021).

[30] B. Kannan, A. Almanakly, Y. Sung, A. Di Paolo, D. A. Rower, J. Braumüller, A. Melville, B. M. Niedzielski, A. Karamlou, K. Serniak *et al.*, Nat. Phys. (2023).

[31] P.-O. Guimond, B. Vermersch, M. L. Juan, A. Sharafiev, G. Kirchmair, and P. Zoller, npj Quantum Inf. **6**, 32 (2020).

[32] N. Gheeraert, S. Kono, and Y. Nakamura, Phys. Rev. A **102**, 053720 (2020).

[33] X. Yang, W. Zheng, Z. Han, D. Lan, and Y. Yu, Commun. Theor. Phys. **73**, 115104 (2021).

[34] L. Du, M.-R. Cai, J.-H. Wu, Z. Wang, and Y. Li, Phys. Rev. A **103**, 053701 (2021).

[35] P. W. Milonni, *An Introduction to Quantum Optics and Quantum Fluctuations* (Oxford University Press, 2019).

[36] P. Meystre and M. Sargent, *Elements of Quantum Optics* (Springer-Verlag, Berlin, 2007).

[37] K. Sinha, P. Meystre, E. A. Goldschmidt, F. K. Fatemi, S. L. Rolson, and P. Solano, Phys. Rev. Lett. **124**, 043603 (2020).

[38] K. Sinha, P. Meystre, and P. Solano, Nanophotonic Materials, Devices, and Systems **11091**, 53 (2019).

[39] K. Sinha, A. González-Tudela, Y. Lu, and P. Solano, Phys. Rev. A **102**, 043718 (2020).

[40] F. Dinc, A. M. Brańczyk, and I. Ercan, Quantum **3**, 213 (2019).

[41] F. Dinc and A. M. Brańczyk, Phys. Rev. Res. **1**, 032042(R) (2019).

[42] P. W. Milonni and P. L. Knight, Phys. Rev. A **10**, 1096 (1974).

[43] S. Longhi, Opt. Lett. **45**, 3297 (2020).

[44] G. Calajó, Y.-L. L. Fang, H. U. Baranger, and F. Ciccarello, Phys. Rev. Lett. **122**, 073601 (2019).

[45] A. Svidzinsky and J.-T. Chang, Phys. Rev. A **77**, 043833 (2008).

[46] J. Kerckhoff, K. Lalumière, B. J. Chapman, A. Blais, and K. W. Lehnert, Phys. Rev. Appl. **4**, 034002 (2015).

[47] Y.-Y. Wang, S. van Geldern, T. Connolly, Y.-X. Wang, A. Shilcusky, A. McDonald, A. A. Clerk, and C. Wang, arXiv:2106.11283 [quant-ph] (2021).

[48] Q. Wang, Z. Ouyang, M. Lin, and Q. Liu, Appl. Opt. **54**, 9741 (2015).

[49] D. Huang, P. Pintus, C. Zhang, P. Morton, Y. Shoji, T. Mizumoto, and J. E. Bowers, Optica **4**, 23 (2017).

[50] A. S. Sheremet, M. I. Petrov, I. V. Iorsh, A. V. Poshakinskiy, and A. N. Poddubny, arXiv:2103.06824 [quant-ph] (2021).

[51] N. A. Masluk, I. M. Pop, A. Kamal, Z. K. Minev, and M. H. Devoret, Phys. Rev. Lett. **109**, 137002 (2012).

[52] R. Kuzmin, N. Mehta, N. Grabon, R. Mencia, and V. E. Manucharyan, npj Quantum Inf. **5**, 20 (2019).

[53] S. Léger, J. Puertas-Martínez, K. Bharadwaj, R. Dassonneville, J. Delaforce, F. Foroughi, V. Milchakov, L. Planat, O. Buisson, C. Naud *et al.*, Nat. Commun. **10**, 5259 (2019).

[54] W. L. Lama, R. Jodoin, and L. Mandel, Am. J. Phys. **40**, 32 (1972).

[55] D. Yang, S.-h. Oh, J. Han, G. Son, J. Kim, J. Kim, M. Lee, and K. An, Nat. Photonics **15**, 272 (2021).

[56] M. Zens and S. Rotter, Nat. Photonics **15**, 251 (2021).

[57] H. J. Kimble, Nature (London) **453**, 1023 (2008).

[58] R. J. Schoelkopf and S. M. Girvin, Nature (London) **451**, 664 (2008).

[59] G. Crowder, H. Carmichael, and S. Hughes, Phys. Rev. A **101**, 023807 (2020).

[60] S. Arranz Regidor, G. Crowder, H. Carmichael, and S. Hughes, Phys. Rev. Res. **3**, 023030 (2021).

[61] A. E. Kaplan and P. Meystre, Opt. Lett. **6**, 590 (1981).

[62] A. Kaplan and P. Meystre, Opt. Commun. **40**, 229 (1982).

[63] A. Rosario Hamann, C. Müller, M. Jerger, M. Zanner, J. Combes, M. Pletyukhov, M. Weides, T. M. Stace, and A. Fedorov, Phys. Rev. Lett. **121**, 123601 (2018).

[64] R. M. Corless, G. H. Gonnet, D. E. G. Hare, D. J. Jeffrey, and D. E. Knuth, Adv. Comput. Math. **5**, 329 (1996).